

CHRONOS: Cryogenic sub-Hz cROss torsion bar detector with quantum NON-demolition Speed meter

Yuki Inoue,^{1,2,3,4,*} Hsiang-Chieh Hsu,³ Hsiang-Yu Huang,^{1,2} M.Afif Ismail,^{1,2,3} Vvek Kumar,^{3,5} Miftahul Ma'arif,^{1,2} Avani Patel,^{1,2} Daiki Tanabe,^{3,2,4} Henry Tsz-King Wong,^{3,2} and Ta-Chun Yu^{1,2}

¹*Department of Physics, National Central University, Taoyuan, Taiwan*

²*Center for High Energy and High Field (CHiP), National Central University, Taoyuan, Taiwan*

³*Institute of Physics, Academia Sinica, Taipei, Taiwan*

⁴*Institute of Particle and Nuclear Studies, High Energy Acceleration Research Organization (KEK), Tsukuba, Japan*

⁵*Department of Physics, Institute of Applied Sciences and Humanities, GLA University, Mathura 281406, India.*

(Dated: October 28, 2025)

We propose a next-generation ground-based gravitational-wave detector, the Cryogenic sub-Hz cROss torsion-bar detector with quantum NON-demolition Speed meter (CHRONOS), optimized for the unexplored 0.1–10 Hz band between the space-based LISA and future ground-based detectors such as Cosmic Explorer and the Einstein Telescope. CHRONOS combines a ring-cavity Sagnac interferometer with torsion-bar test masses to realize the first quantum nondemolition (QND) measurement of angular momentum in a macroscopic system. By implementing a speed-meter readout in the rotational degree of freedom, CHRONOS coherently cancels quantum radiation-pressure noise and enables sub-Hz observations. We calculate, for the first time, that detuned power recycling and cavity-length optimization can simultaneously relax technical requirements on both the torsion bars and the speed meters. Assuming a realistic optical design with a 1 m torsion bar, we estimate strain sensitivities of $h \simeq 1 \times 10^{-18} \text{ Hz}^{-1/2}$ at 1 Hz for detectors with arm lengths of 2.5 m, 40 m, and 300 m. These sensitivities enable (i) the direct detection of intermediate-mass black hole binaries out to 380 Mpc with $\text{SNR} = 3$, and (ii) the probing of stochastic gravitational-wave backgrounds down to $\Omega_{\text{GW}} \sim 3.2 \times 10^{-9}$ at 0.2 Hz with five years of data accumulation. Furthermore, CHRONOS enables the prompt detection of gravity-gradient signals from $M = 5.5$ earthquakes even with a 2.5 m prototype. CHRONOS thus opens new opportunities for quantum-limited geophysical observation and for multi-band, multi-messenger gravitational-wave astronomy.

I. INTRODUCTION

The first direct detection of gravitational waves by LIGO [1] opened the era of gravitational-wave astronomy, followed by Virgo [2] and KAGRA [3], which operate above 10 Hz and have provided key insights into compact binaries and fundamental physics. At much lower frequencies, space-based missions such as LISA [4] will explore the millihertz band (10^{-4} – 10^{-1} Hz), targeting supermassive black hole mergers and cosmological signals.

However, the intermediate range of ~ 0.1 –10 Hz remains largely unexplored despite its rich science potential, including intermediate-mass black hole (IMBH) binaries, stochastic gravitational-wave backgrounds (SGWBs), and prompt gravity-gradient signals from seismic events. Bridging this sensitivity gap requires fundamentally new detection principles.

Torsion-bar-based detectors such as TOBA [5] and TorPeDO [6] demonstrated sub-Hz feasibility but the fundamental quantum back-action limits in displacement readout, requiring massive test masses for ensuring sensitivity below 1 Hz [5].

We propose Cryogenic sub-Hz cROss torsion-bar detector with quantum NON-demolition Speed meter (CHRONOS), a next-generation detector combining a triangular Sagnac interferometer with torsion-bar test masses to realize the first quantum nondemolition (QND) measurement of angular momentum in a macroscopic system [7, 8]. QND is a system that can break the trade-off between shot noise and back-action noise arising from quantum commutation relations, and it has been reported that this can be realized through squeezing techniques [9, 10] and speed meters [11–13].

A novel speed-meter readout cancels radiation-pressure noise, and power-recycling mirror detuning further suppresses the low-frequency noise with coating losses. These issues represent technical challenges for enhancing the sensitivity of torsion bars and for the first demonstration of a speed meter, and addressing them with a speed meter and a dual-recycled torsion-bar system is a unique approach.

In this paper, we explicitly evaluate the sensitivity for different test facility scales: a 2.5 m arm length, corresponding to a Glasgow-type 10 m interferometer [14]; a 40 m arm length [15], corresponding to the Caltech 40 m interferometer; and a 300 m arm length, corresponding to the TAMA300 [16–18].

* Corresponding author: iyuki@ncu.edu.tw

II. DETECTOR CONCEPT

The CHRONOS detector introduces a new paradigm for low-frequency gravitational-wave detection by combining torsion-bar test masses, triangular ring cavities, and a dual-recycled Sagnac interferometer. Torsion-based detectors such as TOBA [5] and TorPeDO [6] have demonstrated sub-Hz angular displacement measurements θ by exploiting correlated torsion-bar motion. In these systems, the response of a torsion bar in the x - y plane with moment of inertia $I = \int \rho(x^2 + y^2)dV$ is $\theta(\Omega) = \eta(h_+F_+ + h_\times F_\times)$, where $h_{+,\times}$ are gravitational-wave polarizations, $F_{+,\times}$ are antenna patterns, and geometrical factor $\eta = I / \int \rho(x^2 - y^2)dV$, with ρ and V denoting the test-mass density and volume. Ω is the signal sideband frequency. For all cases, we assume identical torsion-bar geometries with length of torsion bar $L_{bar} = 1$ m, moment of inertia $I = 19.9$ kg m², test-mass mass $M = 171$ kg, test-mass temperature $T = 10$ K and a geometrical factor $\eta = 0.936$. Assuming the torsional resonance lies well below the observation band, these schemes are fundamentally limited by quantum radiation-pressure back-action noise below 1 Hz.

Figure 1 shows the CHRONOS optical configuration. Two orthogonal torsion bars are suspended in a cross geometry, each hosting a triangular ring-cavity. After pre-isolation, the input beam passes through an input mode cleaner and is split at the input beam splitter (IBS). The beams enter the X and Y arms, each forming a dual-recycled speed-meter cavity with a power-recycling mirror (PRM, PR1) and signal-recycling mirror (SRM, SR1). Outputs are recombined at the output beam splitter (OBS), filtered by an output mode cleaner, and read out via balanced homodyne detection. The detailed optical design of CHRONOS is described in Inoue *et al* [19]. As the X and Y arms are identical, we focus on the Y arm below.

CHRONOS overcomes differential angle readout limitations by directly measuring the conjugate angular momentum L , enabling the first QND measurement of L in macroscopic system with O(100kg) test masses. Using counter-propagating beams in the triangular cavity formed by ETMLY–MTMLY–ITMLY and ETMRY–MTMRY–ITMRY as shown in Fig. 1, separated at BSY, the optical delay between beams gives direct access to $L(t) \propto (\theta(t + \tau) - \theta(t))/\tau$, where τ is the optical path delay. For conventional differential angle readout, $\dot{\theta} = [\hat{H}, \hat{\theta}] \neq 0$ implies future θ evolves under back-action, whereas $\dot{L} = [\hat{H}, \hat{L}] = 0$ ensures L remains unaffected. Thus, $[\hat{L}(t), \hat{L}(t')] = 0$, demonstrating that L is a QND observable.

QND is a system that can break the trade-off between shot noise and back-action noise arising from quantum commutation relations, and it has been reported that this can be realized through squeezing techniques [7, 9, 10] and speed meters [8, 12, 13]. By circumventing the quantum trade-off between shot noise and radiation-pressure noise [20, 21], these approaches provide a unique pathway toward surpassing the conventional quantum limits in gravitational-wave detectors.

III. NOISE BUDGET AND SENSITIVITY

We evaluate the sensitivity of CHRONOS using both an analytical quantum-operator approach and full simulations performed with FINESSE3 [22]. The unique aspects of this study are the implementation of power recycling cavity (PRC) detuning and the integration of a speed-meter topology with torsion-bar test masses. Balanced homodyne detection is assumed throughout [23].

Following the generalized framework of Buonanno and Chen [24–28], incorporating detuning terms for both the power-recycling cavity (PRC) and the signal-recycling cavity (SRC), the angular displacement noise can be expressed as

$$\theta = \frac{\theta_{\text{SQL}}}{\sqrt{2(1 - r_s^2)\kappa_{\text{sag}}}} \sqrt{\frac{\boldsymbol{\nu}^\top G \boldsymbol{\nu}}{\boldsymbol{\nu}^\top Q \boldsymbol{\nu}}}, \quad (1)$$

where $\theta_{\text{SQL}} = \sqrt{2\hbar/(I\Omega^2)}$ is the standard quantum limit (SQL) of angular displacement noise [5]. $\boldsymbol{\nu}^\top = (\cos \zeta, \sin \zeta)$ is the homodyne detection vector, defined by the readout angle ζ . r_s is the amplitude reflectivity of the signal-recycling mirror. We define $G = CC^\top$, and $Q = \Re(\mathbf{D})\Re(\mathbf{D})^\top + \Im(\mathbf{D})\Im(\mathbf{D})^\top$.

Here, the matrix $C = [c_{ij}]$ and the column vector $\mathbf{D}^\top = (D_1, D_2)$ are defined following Eqs. (2.22)–(2.24) of Ref. [24]. The optomechanical coupling factor κ defined in [24, 26, 29, 30] is modified as $\kappa_{\text{sag}} = 4\kappa |H_{\text{PRC}}|^2 \sin^2 \beta_{\text{sag}}$, where

$$H_{\text{PRC}} = \frac{t_p}{1 - ir_p|r_{\text{ifo}}|\sin \beta_{\text{sag}}e^{2i(\phi_p + \tau_p\Omega)}}, \quad (2)$$

and the effective Sagnac phase shift is $\beta_{\text{sag}} = 2\beta + \pi/2$ [31]. β is the single-pass phase accumulated by the signal sideband in the arm cavity. t_p and r_p are amplitude transmission and reflection coefficients of the PRC mirror. r_{ifo}

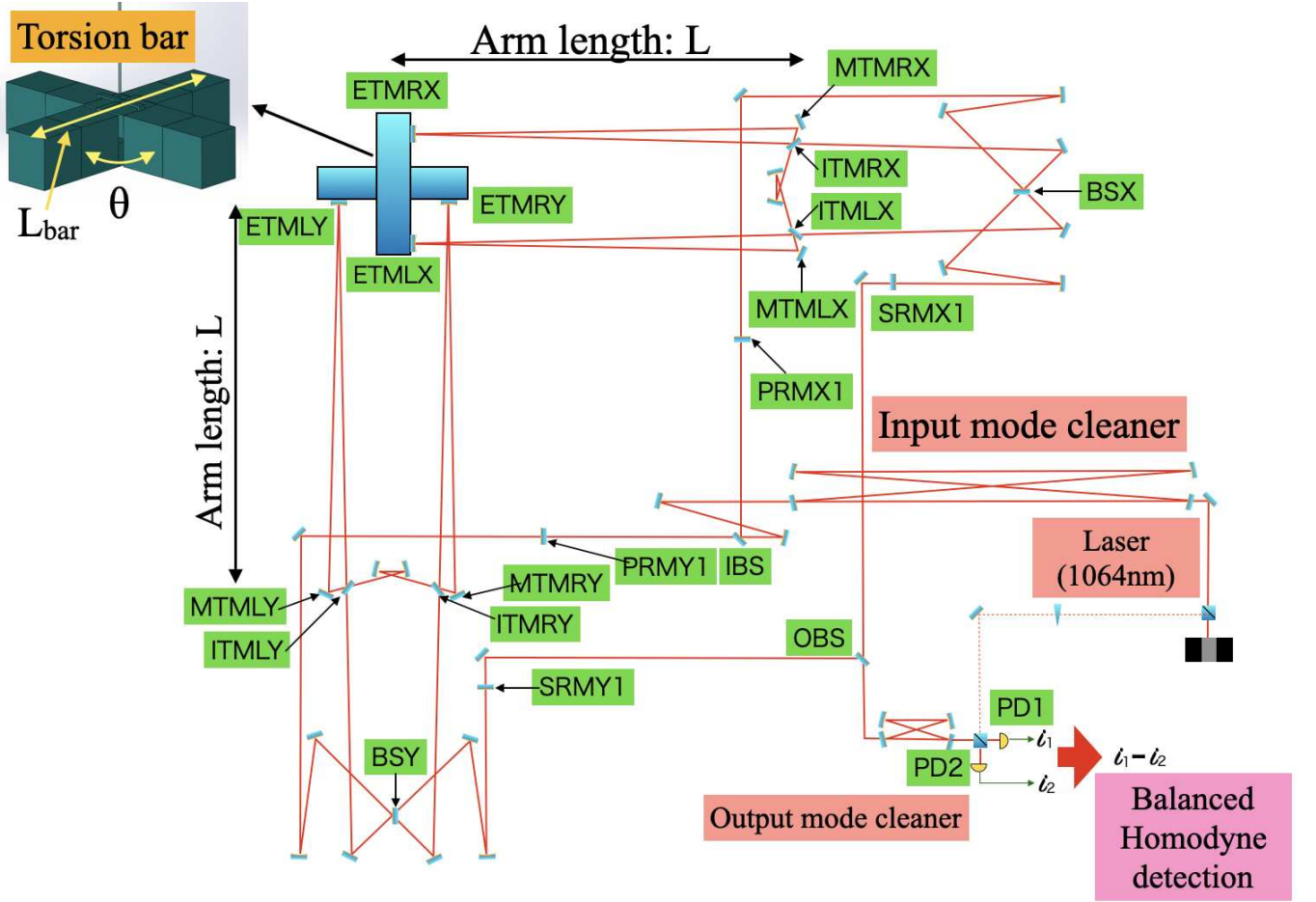


Figure 1: Optical configuration of CHRONOS. The Sagnac interferometer integrates: (i) torsion-bar test masses at the center, (ii) Ring cavity with Sagnac interferometer at both arm, (iii) dual-recycled cavities with SRM and PRM.

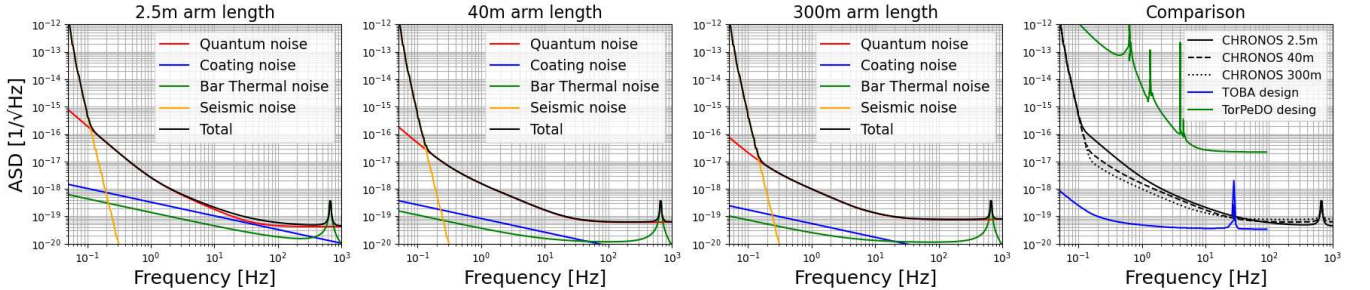


Figure 2: Predicted CHRONOS strain sensitivity (black) and dominant noise contributions. Quantum noise is calculated with sum of shot noise and radiation noise.

is the effective complex reflectivity of the interferometer, including SRC detuning and internal losses. ϕ_p is PRC detuning phase. τ_p is one-way propagation time in the PRC.

The above expression can be diagonalized along the principal axes:

$$\theta = \frac{\theta_{\text{SQL}}}{\sqrt{2}\Gamma(\phi_s, \zeta)\kappa_{\text{sag}}} \sqrt{1 + (\cot \zeta_{\text{eff}} - \kappa_{\text{eff}})^2}, \quad (3)$$

where

$$\Gamma(\phi_s, \zeta) = (1 - r_s^2) \sqrt{|D_1|^2 |D_2|^2 - \Re(D_1 D_2^*)^2}, \quad (4)$$

and the effective optomechanical coupling derived from G and Q is

$$\kappa_{\text{eff}} = \sqrt{\frac{Q_{22}G_{11} + Q_{11}G_{22} - 2Q_{12}G_{12}}{\sqrt{\det Q} \sqrt{\det G}}} - 2. \quad (5)$$

The effective homodyne angle is given by $\zeta_{\text{eff}} = \zeta - \psi(f) + \theta(f)$, where $\psi(f)$ and $\theta(f)$ denote the principal-axis rotations of G and Q , respectively.

We estimate the strain sensitivity for three detector scales optimized for the sub-Hz regime, where the sensitivity is tuned to peak at 1 Hz. The interferometer parameters used in the calculation are summarized in Table I, and the resulting sensitivity curves are shown in Fig. 2.

Table I: Interferometer parameters for sensitivity estimates.

	2.5 m	40 m	300 m
$R_s/R_p/R_i$	0.5/0.9/0.9999	0.5/0.95/0.999	0.5/0.99/0.995
$P_{\text{in}}/P_{\text{arm}}$	1W / 444W	20W / 2391W	100W / 18.3kW
$\phi_p/\phi_s/\zeta$	-85 / 0 / 46	26 / 0 / -50	41 / 2 / -66
F_{ring}	3.14×10^4	3.14×10^3	6.27×10^2
w at ETM	2 mm	30 mm	70 mm

Definitions: $R_i = r_i^2$, $R_p = r_p^2$, $R_s = r_s^2$, P_{in} input power, P_{arm} arm power, ϕ_p PRC detuning, ϕ_s SRC detuning, ζ homodyne angle, F_{ring} finesse, w beam radius at ETM.

CHRONOS is optimized for the previously unexplored 0.1–10 Hz band. Extending the arm length shifts the radiation-pressure noise crossover frequency toward lower frequencies, enhancing low-frequency performance. Assuming a coating loss of 0.1 ppm, quantum noise is strongly suppressed compared to conventional designs; in an ideal lossless system, the suppression is even more significant. Increasing the arm length also improves the effective optical delay τ while reducing the required finesse, thereby relaxing coating-loss requirements.

A key feature of CHRONOS is its use of PRC detuning in Eq. (2), which differs from the conventional approach of detuning the SRM. Focusing on the PRC transfer function, the detuning angle of the PRC acts simultaneously on both the clockwise (CW) and counter-clockwise (CCW) components of the Sagnac speed meter [31]. This phase shift propagates into the effective homodyne angle, ζ_{eff} as a term $\arg(H_{\text{prc}})$, so by controlling the frequency-dependent phase balance of the CW and CCW beams through the PRC, one can effectively impart a frequency-dependent homodyne angle. In addition to enhancing the carrier field and increasing circulating power, PRC detuning enables sensitivity shaping with engineered frequency dependence, thereby suppressing radiation-pressure noise and reducing shot noise.

Furthermore, integrating the PRM and SRM into a coupled cavity enhances the equivalent optical delay τ and relaxes the stringent optical-loss requirement of speed-meter topologies from 0.01 ppm to a practical level of 0.1 ppm. With these techniques combined, CHRONOS achieves a target sensitivity of $h \simeq 1 \times 10^{-18} \text{ Hz}^{-1/2}$ around $f \sim 1 \text{ Hz}$.

IV. SCIENTIFIC REACH

Three science packages are discussed for the scientific outcomes assuming each corresponding sensitivity as follows.

First, CHRONOS targets merger signals from IMBH binaries with component masses of 1×10^2 – $5 \times 10^5 M_\odot$ [4, 32–34]. These signals enter the CHRONOS band weeks to days before coalescence, enabling multi-band observations in synergy with LISA and future detectors such as Voyager, Cosmic Explorer, and the Einstein Telescope [1, 4]. For $M \sim 10^3 M_\odot$, CHRONOS can detect mergers up to 380 Mpc at $\text{SNR} = 3$, allowing the first statistical studies of IMBH populations and insights into supermassive black hole formation as shown in Fig. 3. Moreover, at low frequencies, the use of high-finesse cavities causes coating losses that can destroy the QND system. This effect corresponds to the achievable finesse and the time delay τ , but by increasing the arm length, an equivalent time delay can be realized with fewer reflections. As a result, low-frequency QND measurements can be maintained, leading to an increased SNR for high-mass IMBH binaries.

Second, CHRONOS bridges the sensitivity gap between LISA [4] and ground-based detectors [1], enabling strong constraints on the SGWB in the 0.1–10 Hz band. Astrophysical foregrounds include unresolved black hole and neutron star binaries, while cosmological sources may arise from first-order phase transitions, cosmic strings, primordial black holes, and inflationary relics [35]. Figure 4 shows the predicted sensitivities by assuming five year of integration. CHRONOS achieves an energy-density sensitivity of $\Omega_{\text{GW}} \sim 3.2 \times 10^{-9}$ at 0.2 Hz, enabling new constraints on the search of new stochastic background source, such as primordial black holes.

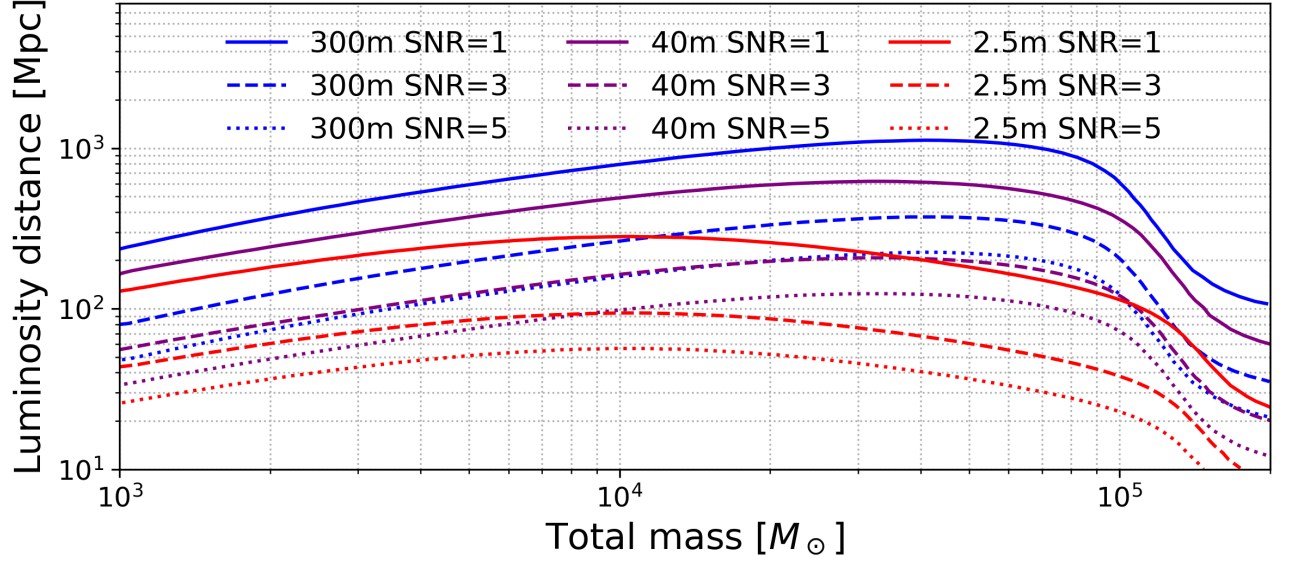


Figure 3: Estimated signal-to-noise ratios for IMBH binary mergers with CHRONOS.

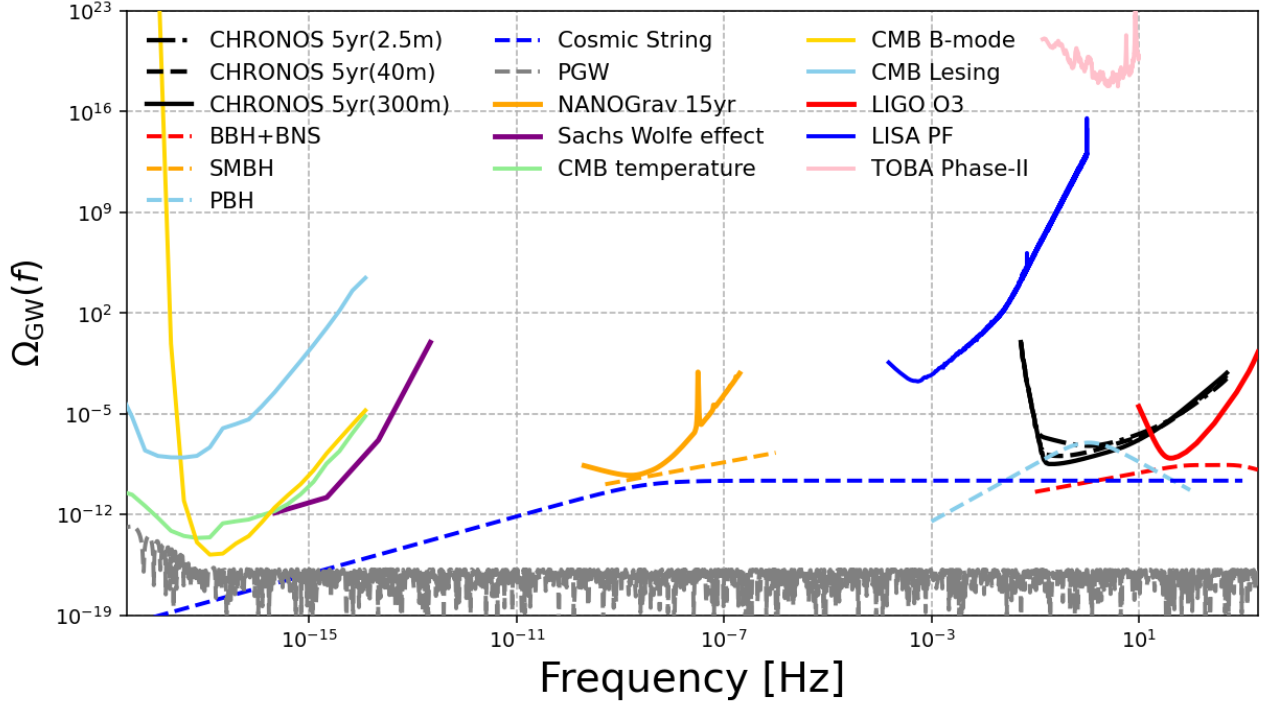


Figure 4: Expected sensitivity of CHRONOS to the SGWB. LIGO O3 [36], LISA pathfinder [37], Sachs Wolfe effect [38], CMB B-mode ($r < 0.06$), CMB Lensing, CMB Temperature [39], show the current observational limit. Binary blackhole and Binary Neutron star (BBH+BNS) [40], Super massive blackhole (SMBH) [41], Primordial Blackhole (PBH, $\chi^* = 100$) [42, 43], Nambu-Goto type Cosmic string ($G\mu \sim 10^{-8}$, $\sigma = 0.1$) [44–46], with Primordial Gravitational Wave (PGW) [41] are theoretical predictions.

Finally, CHRONOS enables detection of prompt gravity-gradient signals from large earthquakes as shown in Fig 5. These signals arise from rapid mass redistribution and propagate at the speed of light, potentially allowing detection seconds before destructive surface waves [47–49]. Simulations for the ASGRAF [50] site near Taipei show high detection efficiency within a 100 km radius. Taking into account the density of the ground, the minimum duration time of the arrived surface wave is estimated to be 8.3 sec. By applying immediate analysis with the front-end system and IIR-based reconstruction [51, 52], as used in gravitational-wave detector calibration, in principle the

seismic disturbance can be identified within $O(100 \mu\text{s})$, corresponding to the sum of clock time and the speed of light transmission [47, 48, 53]. paving the way for ultra-rapid earthquake early-warning systems using gravitational measurements.

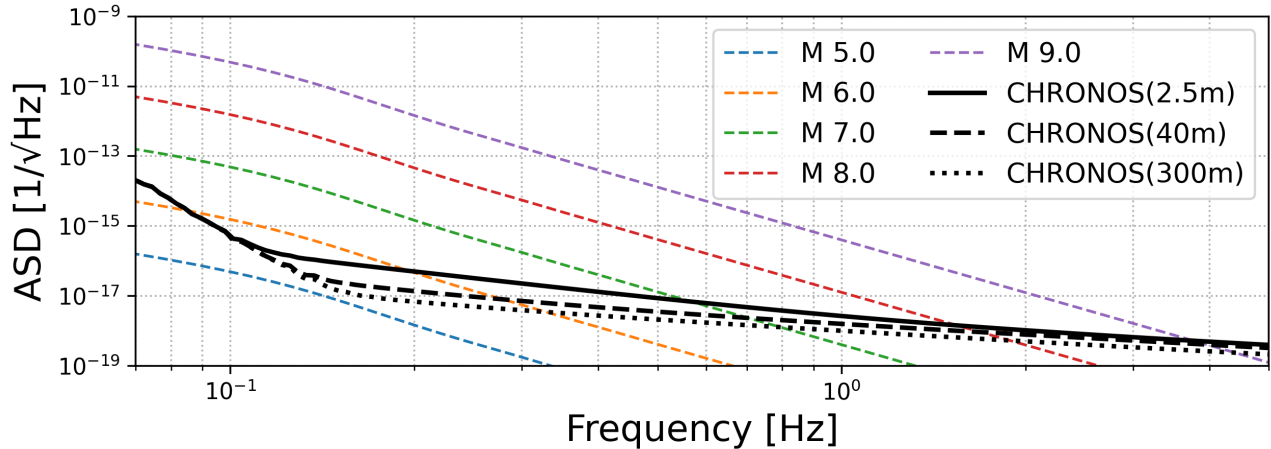


Figure 5: Predicted sensitivity to prompt gravity signals from large earthquakes. By detecting gravitational perturbations at the speed of light, CHRONOS enables warnings before surface-wave arrival.

V. DISCUSSION

We investigated how QND techniques can enhance torsion-bar gravitational-wave detectors. By independently reading out each torsion bar and taking their differential signal, CHRONOS suppresses common-mode noise such as translation, bulk deformation, and laser intensity fluctuations as described in Tanabe *et al* [54]. The sapphire test mass is assumed with 22 cm mirrors identical to KAGRA [55], with connection by hydro-catalysis bonding [56]. Cryogenic operation relaxes bonding Q requirements and suppresses thermal lensing without extreme laser power or finesse. In the future, we expect more precise measurements from CMB projects [57, 61], Pulsar Timing Array [?] [Dewdney2009SKA], and interferometers [58–60]. With them, the importance of the CHRONOS measurements will be further enhanced.

VI. CONCLUSION

We have presented the design concept of CHRONOS, a next-generation ground-based gravitational-wave detector optimized for the unexplored 0.1–10 Hz band. By combining a triangular Sagnac interferometer with torsion-bar test masses, CHRONOS expects to achieve the first QND measurement of angular momentum in a macroscopic system [10, 31]. This speed-meter readout suppresses quantum radiation-pressure noise, enabling sub-Hz sensitivity. With a target sensitivity of $h \simeq 1 \times 10^{-18} \text{ Hz}^{-1/2}$ at $f \sim 1 \text{ Hz}$, CHRONOS will open a new window for gravitational-wave astronomy. It enables detection of intermediate-mass black hole binaries [32], probing stochastic backgrounds from the early universe [41, 61], and detecting prompt gravity signals from large earthquakes [47–49]. By bridging the gap between LISA [4] and future detectors such as Voyager and the Einstein Telescope [62, 63], CHRONOS will establish a crucial platform for multi-band gravitational-wave and multi-messenger astronomy.

ACKNOWLEDGMENTS

We thank S.Takano, M.Ando and T.Namikawa for providing the TOBA data and CMB data. We also thank K.W.Ng and M.Hazumi for their academic advice during the preparation of this manuscript. We thank M.Hasegawa, T.Kanayama, S.Matsushita, H.Murakami, M.Inoue, R. Shibuya and C.M.Kuo for support to establish CHRONOS team. Y.I. and H.W. acknowledges support from NSTC, CHiP, GSROC and Academia Sinica in Taiwan under Grant

No.114-2112-M-008-006-, and No.AS-TP-112-M01.

-
- [1] B. P. Abbott *et al.* (LIGO Scientific Collaboration and Virgo Collaboration), *Phys. Rev. Lett.* **116**, 061102 (2016).
 - [2] F. Acernese *et al.* (Virgo Collaboration), *Class. Quantum Grav.* **32**, 024001 (2015).
 - [3] T. Akutsu *et al.* (KAGRA Collaboration), *Prog. Theor. Exp. Phys.* **2021**, 05A101 (2021).
 - [4] P. Amaro-Seoane *et al.*, arXiv:1702.00786 (2017).
 - [5] M. Ando *et al.*, *Physical Review Letters* **105**, 161101 (2010).
 - [6] L. Ju, C. Zhao, and D. Blair, in *Proceedings of the 13th Marcel Grossmann Meeting* (2019) pp. 2487–2492.
 - [7] C. M. Caves, K. S. Thorne, R. W. P. Drever, V. D. Sandberg, and M. Zimmermann, *Reviews of Modern Physics* **52**, 341 (1980).
 - [8] V. B. Braginsky, Y. I. Vorontsov, and K. S. Thorne, *Science* **209**, 547 (1980).
 - [9] V. B. Braginsky and F. Y. Khalili, *Quantum Measurement* (Cambridge University Press, 1996).
 - [10] S. L. Danilishin and F. Y. Khalili, *Living Rev. Relativ.* **15**, 5 (2012).
 - [11] V. B. Braginsky and F. Y. Khalili, *Phys. Lett. A* **147**, 251 (1990).
 - [12] P. Purdue and Y. Chen, *Physical Review D* **66**, 122004 (2002).
 - [13] F. Y. Khalili, *Physics Letters A* **298**, 308 (2002).
 - [14] D. I. Robertson, E. Morrison, J. Hough, S. Killbourn, B. J. Meers, G. P. Newton, N. A. Robertson, K. A. Strain, and H. Ward, *Review of Scientific Instruments* **66**, 4447 (1995).
 - [15] E. Chase, *Detector Characterization of the LIGO 40 m Prototype Interferometer*, Tech. Rep. LIGO-T1500123 (LIGO / Caltech / MIT, 2015).
 - [16] M. Ando and the TAMA Collaboration, arXiv preprint arXiv:astro-ph/0105473 (2001), [astro-ph/0105473](#).
 - [17] D. Tatsumi and the TAMA Collaboration (2008).
 - [18] L. S. Collaboration and T. Collaboration, arXiv preprint arXiv:gr-qc/0507081 (2005), [gr-qc/0507081](#).
 - [19] Y. Inoue *et al.* (2025), in preparation.
 - [20] M. Ozawa, *Physical Review A* **67**, 042105 (2003).
 - [21] M. Ozawa, *Annals of Physics* **311**, 350 (2004).
 - [22] D. D. Brown, A. Freise, *et al.*, *SoftwareX* **14**, 100678 (2021).
 - [23] R. X. Adhikari, *Rev. Mod. Phys.* **86**, 121 (2014).
 - [24] A. Buonanno and Y. Chen, *Physical Review D* **64**, 042006 (2001), arXiv:gr-qc/0102012.
 - [25] A. Buonanno and Y. Chen, *Physical Review D* **65**, 042001 (2002), arXiv:gr-qc/0107021.
 - [26] Y. Chen, *Physical Review D* **67**, 122004 (2003), arXiv:gr-qc/0208051.
 - [27] K. Yamamoto, M. Ando, K. Kawabe, *et al.*, *Physical Review A* **81**, 033849 (2010), arXiv:0912.2603 [quant-ph].
 - [28] P. Purdue, *Phys. Rev. D* **66**, 10.1103/PhysRevD.66.022001 (2002), arXiv:gr-qc/0111042 [gr-qc].
 - [29] S. L. Danilishin and F. Y. Khalili, *Living Reviews in Relativity* **15**, 5 (2012).
 - [30] C. Gräf, B. Barr, A. S. Bell, S. L. Danilishin, *et al.*, *Classical and Quantum Gravity* **31**, 215009 (2014), arXiv:1405.2783 [gr-qc].
 - [31] Y. Chen, *Phys. Rev. D* **67**, 122004 (2003).
 - [32] A. Sesana, *Phys. Rev. Lett.* **116**, 231102 (2016).
 - [33] M. C. Miller, *Astrophys. J.* **618**, 426 (2004).
 - [34] P. Amaro-Seoane, in *J. Phys. Conf. Ser.*, Vol. 840 (2017) p. 012002.
 - [35] N. Christensen, *Rep. Prog. Phys.* **82**, 016903 (2019).
 - [36] R. Abbott *et al.*, *Phys. Rev. D* **104**, 022004 (2021), arXiv:2101.12130 [gr-qc].
 - [37] G. Boileau, N. Christensen, and R. Meyer, *Phys. Rev. D* **106**, 063025 (2022), arXiv:2204.03867 [gr-qc].
 - [38] K. W. Ng, *Phys. Rev. D* **106**, 043505 (2022), arXiv:2106.12843 [astro-ph.CO].
 - [39] T. Namikawa, S. Saga, D. Yamauchi, and A. Taruya, *Phys. Rev. D* **100**, 021303 (2019).
 - [40] The-LIGO-Scientific-Collaboration, *Physical Review D* **100**, 061101 (2019), arXiv:arXiv:1903.02886 [gr-qc].
 - [41] P. Campeti, E. Komatsu, D. Poletti, and C. Baccigalupi, *Journal of Cosmology and Astroparticle Physics* (01), 012, arXiv:arXiv:2007.04241 [astro-ph.CO].
 - [42] K. Kohri and T. Terada, *Phys. Rev. D* **97**, 123532 (2018), arXiv:1804.08577 [astro-ph.CO].
 - [43] G. Domènech, *Universe* **7**, 398 (2021), arXiv:2109.01398 [gr-qc].
 - [44] X. Siemens, V. Mandic, and J. Creighton, *Phys. Rev. D* **73**, 105001 (2006), [astro-ph/0610920](#).
 - [45] J. J. Blanco-Pillado and K. D. Olum, *Phys. Rev. D* **96**, 104046 (2017).
 - [46] P. Auclair *et al.*, *JCAP* (04), 034, 1909.00819.
 - [47] J. Harms, S. Dorsher, H. J. Paik, and M. Venkateswara, *Living Reviews in Relativity* **18**, 10.1007/lrr-2015-3 (2015).
 - [48] J.-P. Montagner, K. Juhel, M. Barsuglia, *et al.*, *Nat. Commun.* **7**, 13349 (2016).
 - [49] M. Vallée, J.-P. Ampuero, K. Juhel, *et al.*, *Science* **358**, 1164 (2017).
 - [50] Academia Sinica GRAvitational research Facility (ASGRAf), <https://www.phys.sinica.edu.tw/~gravitation-physics/research.html>, accessed: 2025-09-26.
 - [51] C. Cahillane, G. Mansell, C. Blair, and et al., *Phys. Rev. D* **102**, 062003 (2020), arXiv:2008.11211 [astro-ph.IM].
 - [52] Y. Inoue *et al.*, *Review of Scientific Instruments* **94**, 054502 (2023), arXiv:2302.12180 [astro-ph.IM].

- [53] L. Ju, J. Harms, and H. Miao, [Nature Reviews Physics](#) **2**, 598 (2020).
- [54] D. Tanabe *et al.* (2025), in preparation.
- [55] T. Ushiba *et al.*, [Classical and Quantum Gravity](#) **36**, 105011 (2019), [arXiv:1902.06645 \[physics.ins-det\]](#).
- [56] E. J. Elliffe, J. Bogenstahl, A. Deshpande, J. Hough, C. J. Killow, S. Reid, N. A. Robertson, S. Rowan, H. Ward, G. Cagnoli, D. R. M. Crooks, P. H. Sneddon, K. A. Strain, J. A. Giaime, K. Mason, R. Route, and P. Willems, [Classical and Quantum Gravity](#) **22**, 257 (2005).
- [57] M. Abitbol *et al.* (Simons Observatory), [JCAP](#) **08**, 034, [arXiv:2503.00636 \[astro-ph.IM\]](#).
- [58] R. X. Adhikari *et al.*, [Classical and Quantum Gravity](#) **37**, 165003 (2020).
- [59] M. Punturo *et al.*, [Classical and Quantum Gravity](#) **27**, 194002 (2010), [arXiv:1002.0461 \[gr-qc\]](#).
- [60] M. Evans *et al.*, [arXiv e-prints](#) (2021), [arXiv:2109.09882 \[gr-qc\]](#).
- [61] E. Allys *et al.* (LiteBIRD), [PTEP](#) **2023**, 042F01 (2023), [arXiv:2202.02773 \[astro-ph.IM\]](#).
- [62] LIGO-Scientific-Collaboration, [LIGO Voyager Concept Study](#), Tech. Rep. (LIGO Laboratory, 2020).
- [63] M. Punturo *et al.*, [The Einstein Telescope: a third-generation gravitational wave observatory](#), Tech. Rep. 19 (ET Science Team, 2010).